NASA TECHNICAL TRANSLATION NASA TT F-14,902

AN INVESTIGATION OF COMPACT RADIO EMISSION SOURCES AT A WAVELENGTH OF 3.55 cm

D. D. Broderick, L. D. Jones, V. L. Efanov,
K. I. Kellermann, B. G. Clark, L. R. Kogan,
V. I. Kostenko, M. N. Cohen, L. I. Matveyenko
and I. G. Moiseyev

Translation of "Issledovaniye kompaktnykh istochnikov kosmicheskogo radioizlucheniya na volne 3,55 CM," Academy of Sciences USSR, Institute of Space Research Report No. Pr-117, Moscow, 1972, 38 pages.

NATIONAL AERONAUTICS AND SPACE ADMINISTRATION
WASHINGTON, D. C. 20546 MAY 1973

AN INVESTIGATION OF COMPACT RADIO EMISSION SOURCES AT A WAVELENGTH OF 3.55 cm

D. D. Broderick, L. D. Jones, V. L. Efanov,
K. I. Kellermann, B. G. Clark, L. R. Kogan,
V. I. Kostenko, M. N. Cohen, L. I. Matveyenko
and I. G. Moiseyev

Unusually active and rapidly varying processes accompanying /3* the liberation of a gigantic amount of energy are encountered in a number of cosmic radio emission sources such as the quasars and the nuclei of radio galaxies. This energy is partially transformed into energy of relativistic particles. The relativisitic electrons are de-excited in magnetic fields and produce powerful radio emission, which permits us to "see" these objects. The energies required to maintain the observed emission are very large. The problem of the origin of this energy and the mechanism for its conversion into relativistic particles is one of the fundamental problems of contemporary astrophysics. The investigation of the physical processes taking place in these objects and the dynamics of their development is associated first of all with the study of their spatial structure. But the angular dimensions of the individual components are unusually small, of the order of one millisecond of arc, and significantly less in a number of cases. Measurements of details of such small dimensions have become possible only in recent years, due to the development of the technique of long-distance interferometry.

*The numbers in the margin indicate pagination of the original foreign text.

Such investigations were carried out by American and Soviet radioastronomers in 1969 at wavelengths of 6 and 2.8 cm [1, 4]. The results of these observations have shown that quasars and the nuclei of galaxies have very complex structures. In a number of cases, individual components were not resolved because of an inadequate baseline or due to insufficient sensitivity. /4

On June 24 - 26, 1971, Soviet-American interferometric observations were carried out on the compact components of quasars and the nuclei of galaxies with the maximum possible baseline under terrestrial conditions at the wavelength of 3.55 cm [3].

The measurements were taken simultaneously with the three radio telescopes: the 22-meter radiotelescope of the Crimean Astrophysical Observatory (KAO of USSR Academy of Sciences) at Simeis, the 42-meter radiotelescope of the National Radio Astronomy Observatory (NRAO) at Green Bank (USA), and the 64-meter radiotelescope of the Deep-Space Network Center of NASA at Goldstone (USA). The limiting angular resolution under terrestrial conditions was achieved at a wavelength of 3.55 cm on the Simeis-Goldstone baseline, which is equal to $270 \cdot 10^6$ λ. The width of an interference fringe was equal to 0".00074. The widths of the fringes on the Simeis-Green Bank and the Green Bank-Goldstone baselines were 0".0009 and 0".002, respectively. A hydrogen frequency standard was used at Goldstone, and a rubidium frequency standard was used at Simeis and at Green Bank.

The tying-in of the time on the radiotelescopes at the start of the observations was accomplished by transporting operating rubidium clocks, and a relative check of the time from day to day was accomplished by means of signals from the Loran C navigational system. Masers were applied with the radiotelescopes at Simeis and at Goldstone, and a parametric amplifier was used at Green Bank.

The new Mark II radio interferometry equipment developed at NRAO (USA) was first used with all three radiotelescopes. The received signals were recorded in digital form on a video magnetic tape at a frequency of $4 \cdot 10^6$ times per second. The magnetic tapes with notations were reduced at Green Bank on a special computer.

Sources were included in the observational program which /5
have compact components at longer wavelengths [1, 4, 5] or which have peculiarities in their spectra at high frequencies and assumed fluxes of the components exceeding the calculated sensitivity. The fluctuation sensitivity of the radio interferometer on the Simeis-Goldstone, Simeis-Green Bank, and the Green Bank-Goldstone baselines was equal to 0.1, 0.35, and 0.08 flux units, respectively.

One of the main difficulties in radio interferometric investigations is the calibration of the instrument. This difficulty arises for a radio interferometer having limiting angular resolution in connection with the absence of calibrated "point" radio sources. Analysis of the results of the present observations has shown that the radio source OJ287 can be adopted as such a source. The amplitude of the interference fringes from this source was identical for all three baselines and did not depend on the hour angle. The determination of the size of the interference fringes' amplitude was carried out on the basis of the internal noises of the system. The noise temperatures of the radiotelescopes were carefully measured at various elevation angles and azimuths. The fluxes of the remaining radio sources were determined with respect to the flux of OJ287. Then corrections were taken into account for variation of the noise texture and the effective antenna area as a function of elevation angle and azimuth. The calibration error evidently results in a change in the correlated components of the sources being investigated

once or a number of times. An estimate of this systematic error shows that it does not exceed 10% (maximum value).

The accidental errors are produced by the following causes:

1. *System noises.* The mean square error in this case, as was pointed out above, equalled 0.1, 0.35, and 0.08 f.u. for the three different baselines. It increased to 20 - 50% for strong radio sources and at low elevation angles. /6

2. *Instability of the heterodynes.* The time of coherent accumulation was selected smaller than the maximum achievable time of averaging for the rubidium standards used in the experiment [6] and equaled ~20 seconds. Due to this circumstance a decrease in the amplitude of the fringes because of instability of the heterodynes is negligibly small. This defect can be neglected even more when the hydrogen frequency standard is used.

3. *Relative error in determining the system noise temperature.* This error does not exceed 3%.

Results of the Observations

The results of the observations of compact components of radio sources are given in Table 1. In the first column of the table are indicated the nomenclature of the source, the size of its total flux F_0 in flux units (1 f.u. = 10^{-26} watts/m^2 Hz) and red shift z; in the second column, the baseline; in the third column, the time of the source observation on the UT scale; in the fourth and fifth columns, the projections of the baseline on the U and V axes in millions of wavelengths; in the sixth column, the correlated component of the flux F_k in flux units; and in the seventh column, the visibility function γ.

TABLE 1 *

/7

Source 1	Baseline 2	UT 3	U 4	V 5	F_k 6	γ 7	Remarks 8
0j 287	GB-CR	I5 06	2I7	-9	3,4±0,6	0,94±0,I6	
F=3,6	GST-CR	I7 42	265	29	3,6±0,4	I,0±0,II	
	GST-GB	I7 4I	59	-I7	3,6±0,4	I,0±0,II	
0R 103	GB-GST	23 36	54,3	-6,2	2,8±0,4	0,94±0,I3	
F=3,0	GB-CR	23.34	2I7	I3	< 2,4	< 0,8	
	GST-CR	23 33	266	22	2,3±0,3	0,77±0,I	
0K290	GB-GST	I7 I9	30	-30	2,I±0,3	I,I7±0,22	
F=1,8		I8 40	56,2	-23,5	I,9±0,3	I,08±0,I5	
	GB-CR	I6 53	225	5	< 2,4	< I,3	
	GST-CR	I7 I3	253	-I5	I,0±0,2	0,56±0,I4	
		I8 40	265	27	0,8±0,2	0,47±0,I5	
00208	GB-GST	2I 47	36,6	-33,6	2,0±0,3	0,80±0,I2	
F=2,5		2I 59	40,9	-32,6	2,2±0,4	0,88±0,I6	
Z=0,077	GB-CR	2I 52	22,3	29	< 2,4	< 0,96	
	GST-CR	2I 53	262	-4	0,75±0,2	0,30±0,08	
VRO422201	GB-GST	8 I4	79,8	-24,2	I2,9±I,5	0,96±0,II	
BL LAC		8 30	82,8	-20,4	I2,5±I,3	0,93±0,I0	
F=I5,6		8 42	84,7	-I7,4	II,9±I,2	0,89±0,09	
	GB-CR	2.53	I85	-75	I2,2±I,6	0,90±0,I2	
		3 07	I93	-68	I2,3±I,7	0,9I±0,I3	
		4 08	2I5	-34	I2,8±I,7	0,95±0,I3	
		4 20	2I8	-26	I3,9±I,8	I,09±0,I3	
		4 3I	22I	-I9	I3,I±I,7	0,97±0,I3	
		4 42	223	-I2	I3,I±I,7	0,97±0,I3	
		4 53	224	-5	I2,6±I,6	0,93±0,I2	

/8

*Commas represent decimal points.

TABLE 1

(Continued)

Source	Baseline	UT	U	V	F_k	γ	Remarks
		5 I2	225	8	I3,0±I,5	0,96±0,I2	
		5 23	225	I4	I2,5±I,6	0,93±0,I2	
		5 37	225	24	II,9±I,5	0,89±0,II	
		5 47	222	3I	II,6±I,5	0,86±0,II	
		5 56	222	37	I2,3±I,6	0,9I±0,I2	
		7 03	200	8I	8,0±I,4	0,59±0,I0	
		7 II	I95	86	7,8±I,2	0,58±0,09	
		8 I3	I6I	II6	6,7±I,I	0,50±0,08	
		8 25	I52	I82	7,0±I,2	0,52±0,09	
		8 33	I47	I25	4,7±0,9	0,35±0,07	
	GST-GR	6 20	265	6	II,9±I,3	0,89±0,I0	
		6 25	265	I0	I2,2±I,3	0,90±0,I0	
		6 3I	266	I5	I2,9±I,4	0,96±0,I0	
		6 36	266	I9	I2,3±I,3	0,9I±0,I0	
		6 4I	266	23	II,7±I,3	0,86±0,I0	
		6 46	265	27	I0,7±I,2	0,79±0,09	
		6 52	265	3I	II,4±I,3	0,85±0,I0	
		6 57	264	35	II,6±I,3	0,86±0,I0	
		7 00	264	37	II,I±I,2	0,82±0,09	
		8 I4	240	92	6,I±0,7	0,45±0,05	
		8 I9	237	96	7,0±0,6	0,52±0,06	
		8 24	235	I00	6,7±0,8	0,50±0,06	
		8 29	232	I03	5,6±0,7	0,4I±0,05	
VRAO-150 F=10,0	G8-GST	9 44	-8,7	-65,8	5,6±0,7	0,63±0,08	11% of the flux is equal to 1.1 f.u.. They refer to components resolved at all our baselines.
		I0 43	I4,8	-55,2	8,0±0,9	0,90±0,I	
		II 33	34,I	-6I,0	7,8±0,8	0,88±0,09	
		I2 I4	46,6	-55,3	8,9±I,0	I,00±0,I	
		I4 06	72,3	-30,4	7,3±0,8	0,82±0,09	
		I4 29	83,5	-24,I	6,6±0,7	0,74±0,08	
		I4 44	85,7	-I9,7	6,I±0,7	0,69±0,08	
		I4 56	87,3	-I6,2	6,I±0,7	0,69±0,08	

19

TABLE 1

(Continued)

Source	Baseline	UT	U	V	F_k	γ	Remarks
	GB-CR	9 32	203	-67	<2,4	<0,27	
		9 42	209	-57	<2,4	<0,27	
		I0 43	224	-I2	<2,4	<0,27	
		II 32	225	25	<2,4	<0,27	
		I2 I5	217	57	<2,4	<0,27	
		I4 06	208	54	<2,4	<0,27	
		I4 38	I38	I47	<2,4	<0,27	
	GST-CR	9 44	200	-I22	2,2±0,3	0,25±0,03	
		I0 44	239	-77	<0,6	<0,07	
		II 33	259	-34	I,I±0,2	0,I2±0,02	
		I2 I4	265	2	I,3±0,2	0,I5±0,02	
		I4 06	243	99	I,5±0,3	0,I7±0,03	
		I4 4I	220	I29	I,6±0,3	0,I8±0,03	
3C 345 $F = 10,2$ $Z = 0,595$	GB-GSI	23 59	27,9	-50	9,2±I	I,03±0,II	$d = \frac{F_k}{9}$ 12% of the flux = 1.2 f.u. They refer to components resolved at all our baselines. /10
		00 I2	32,7	-48,9	8,8±0,9	0,98±0,I0	
		00 3I	39,7	-46,9	8,6±0,9	0,95±0,I0	
		00 44	44,3	-45,5	7,9±0,9	0,87±0,I0	
		0I I5	54,7	-4I,I	7,3±0,9	0,8I±0,I0	
		0I 4I	62,6	-36,9	7,0±0,8	0,78±0,09	
	GB-CR	2I I2	I68	-86	3,9±0,8	0,44 ±0,09	
		2I 34	I83	-74	3,9±0,8	0,44±0,09	
		22 05	I99	-57	4,2±0,9	0,46±0,I0	
		22 30	209	-43	3,3±0,7	0,36±0,08	
		22 48	2I5	-32	3,4±0,7	0,38±0,08	
		23 55	225	I2	4,2±0,9	0,46±0,I0	
		00 06	225	I9	4,2±0,9	0,46±0,I0	
		00 29	223	33	3,7±0,8	0,4I±0,09	
		00 39	22I	40	4,I±0,9	0,45±0,I0	

TABLE 1

(Continued)

Source	Baseline	UT	U	V	F_k	γ	Remarks
		00 I7	224	26	4,I±0,9	0,45±0,I0	
		00 48	2I9	45	4,7±0,9	0,52±0,I0	
		0I 0I	2I6	53	4,2±0,9	0,46±0,I0	
		0I II	2I2	59	4,2±0,9	0,46±0,I0	
		0I 22	209	66	3,6±0,8	0,44±0,09	
		0I 33	204	72	3,7±0,8	0,4I±0,09	
		0I 44	200	79	4,5±I,0	0,50±0,II	
	GST-CR	23 56	252	-38	3,4±0,5	0,38±0,06	
		00 I0	257	-27	3,4±0,5	0,38±0,06	
		0I 03	266	II	2,3±0,4	0,25±0,05	
		0I I4	266	20	2,3±0,4	0,25±0,05	
		0I 24	265	27	2,6±0,5	0,29±0,06	
		0I 35	264	35	2,5±0,5	0,27±0,06	
		0I 45	263	42	2,6±0,5	0,29±0,06	
4C 39.25 F : II,0 Z : 0,7	GST-GB	I5 50	6,8	-5I,7	I0,9±I,5	0,99±0,I4	
		I6 I8	I8,0	-50,7	9,5±I,5	0,86±0,I4	
		I8 I0	58,0	-38,8	8,6±I,5	0,78±0,I4	/11
	GB - CR	I3 48	I63	-88	3,3±0,8	0,3±0,07	
		I4 08	I76	-78	4,7±0,9	0,43±0,08	
		I5 2I	2I2	-38	2,8±0,7	0,25±0,06	
		I5 47	220	-2I	4,I±0,9	0,37±0,08	
		I5 57	222	-I4	4,4±0,9	0,40±0,08	
		I6 09	224	-8	4,I±0,9	0,37±0,08	
		I6 20	225	-I	3,7±0,8	0,34±0,07	
		I6 27	225	4	3,8±0,9	0,36±0,08	
		I8 09	208	66	3,7±0,8	0,34±0,07	
		I8 I7	205	7I	4,7±0,9	0,43±0,08	
	GST-CR	I6 05	236	-60	< 0,8	< 0,07	
		I8 09	265	28	I,I±0,2	0,I±0,02	
		I9 I0	25I	72	< 0,8	< 0,07	

TABLE 1

(Continued)

Source	Baseline	UT	U	V	F_k	γ	Remarks
3C84	GST-GB	9 24	-I	-54,8	I2,3±I,6	0,29±0,04	
F=42,5		I0 I4	I8,9	-53,5	I5,6±I,9	0,37±0,05	
z=0,017		I0 59	36,I	-49,9	I7,9±2,3	0,42±0,05	
		II I6	42,2	-48	I8,6±2,6	0,44±0,06	
		II 20	43,5	-47,5	I8,9±2,6	0,44±0,06	
		II 54	55,0	-42,6	I8,6±2,6	0,44±0,06	
		I2 33	66,5	-35,8	I7,9±2,5	0,42±0,06	
	GB-CR	8 2I	I97	-62	3,0	0,07	
		9 I3	2II	-42	3,9±I,0	0,09±0,02	
		9 25	2I6	-35	3,I±I,I	0,I2±0,03	
		09 54	222	-I6	3,6±I,0	0,08±0,02	
		I0 I3	225	-2	3,6±I,0	0,08±0,02	
		II 08	222	35	3	0,07	
		II 52	2I2	62	3,I±0,9	0,07±0,02	/12
		I2 35	I94	86	3	0,07	
	GST-CR	9 24	2I5	-88	I,7±0,4	0,04±0,0I	
		I0 I2	243	-56	2,5±0,5	0,06±0,0I	
		II 05	26I	-I6	3,2±0,6	0,07±0,0I	
		II I7	263	-7	2,6±0,5	0,06±0,0I	
		II 53	265	20	2,4±0,5	0,06±0,0I	
		I2 32	26I	50	I,8±0,4	0,04±0,0I	
3C273	GB-GST	20 4I	48	4,5	I8,9±2,2	0,6I±0,07	
F=49		20 49	50,6	4,6	I6,I±2	0,52±0,06	
z=0,I58		20 56	52,9	4,6	I3,6±I,8	0,44±0,06	

TABLE 1

(Continued)

Source	Baseline	UT	U	V	F_k	γ	Remarks
	GB-CR	I8 4I	2I7	I2	4,I±I,0	0,I3±0,03	
		I9 II	223	I3	4,7±I,0	0,I5±0,03	
	CR-GST	20 43	265	2I	8,6±I,2	0,28±0,04	
		20 54	265	2I	8,7±I,2	0,28±0,04	
		20 59	266	22	8,7±I,2	0,28±0,04	
3C 120 F=7,6	GST-GB	I3 0I	52,8	0,6	4,3±0,6	0,56±0,08	
Z=0,033	GB-CR	II 29	225	I2	< 2,5	< 0,33	
	GST-CR	I3 0I	266	2I	I,6±0,4	0,2I±0,05	
3C274 F=44	GST-GB	20 22	40,5	-I0,6	I,6±0,4		
Z=0,0041		2I 20	60,0	-7,6	I,8±0,4		
	GB-CR	I9 47	224	I6	< 2,5		
	GST-CR	2I 20	262	I2	< 0,8		

[Commas indicate decimal points; GB — Green Bank; CR — Crimean; GST — Goldstone.]

The total flux densities on the day of the observations were determined from the antenna temperature of the radiotelescope at Goldstone and compared with the results [7]. The source 3C274, whose radio emission flux density does not vary with time [7], was adopted as the reference source. The results of the comparison are shown in Figure 1.

The brightness distributions were calculated on the basis /13
of the observational results obtained. Several models were considered for each source, including ellipses with uniform and Gaussian brightness distributions for different dimensions and orientation of the axes, two- and three-component models with different ratios of the component flux densities, distances

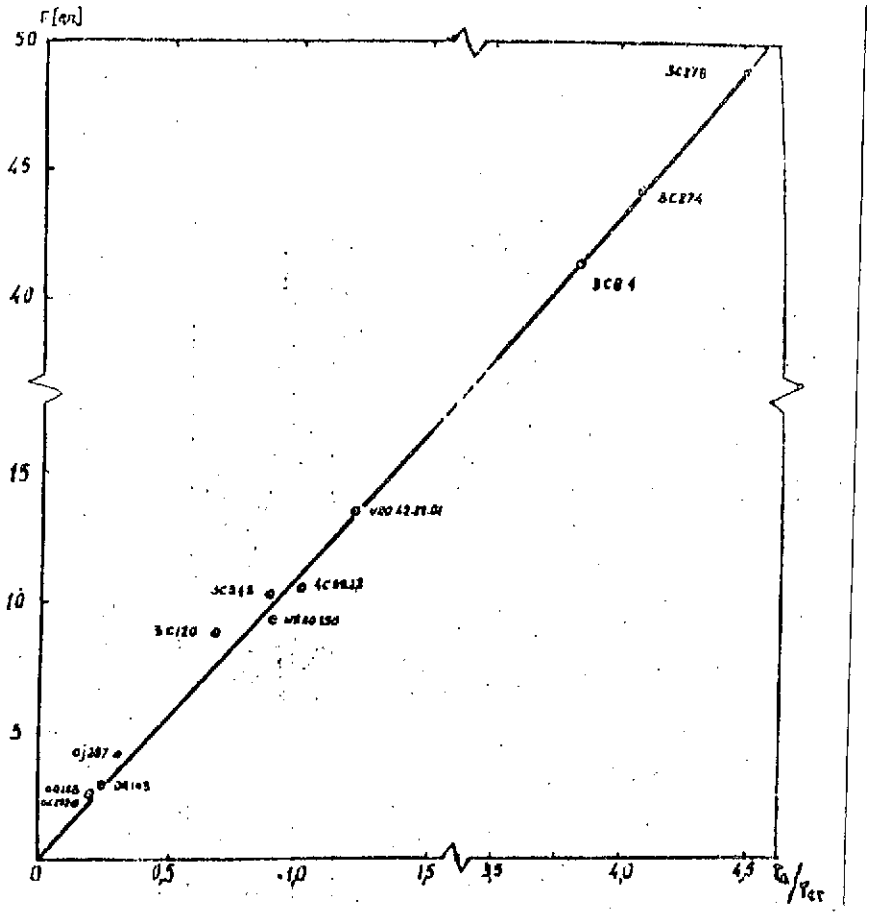

Figure 1. Dependence of the antenna temperature on the radio emission flux density.

between the components, and position angles. Plots of the visibility functions of the models giving the best agreement with the experimental points are given in Figure 2 for some of the sources. The visibility functions are plotted along the ordinate, and the hour angles of the interferometer, figured from its meridian, are plotted along the abscissa on the three graphs corresponding to the three baselines. Photographs of the projections of the baseline vectors onto the U - V plane of the source are shown in the upper right-hand corner. The arrow indicates the direction of increasing hour angle. The

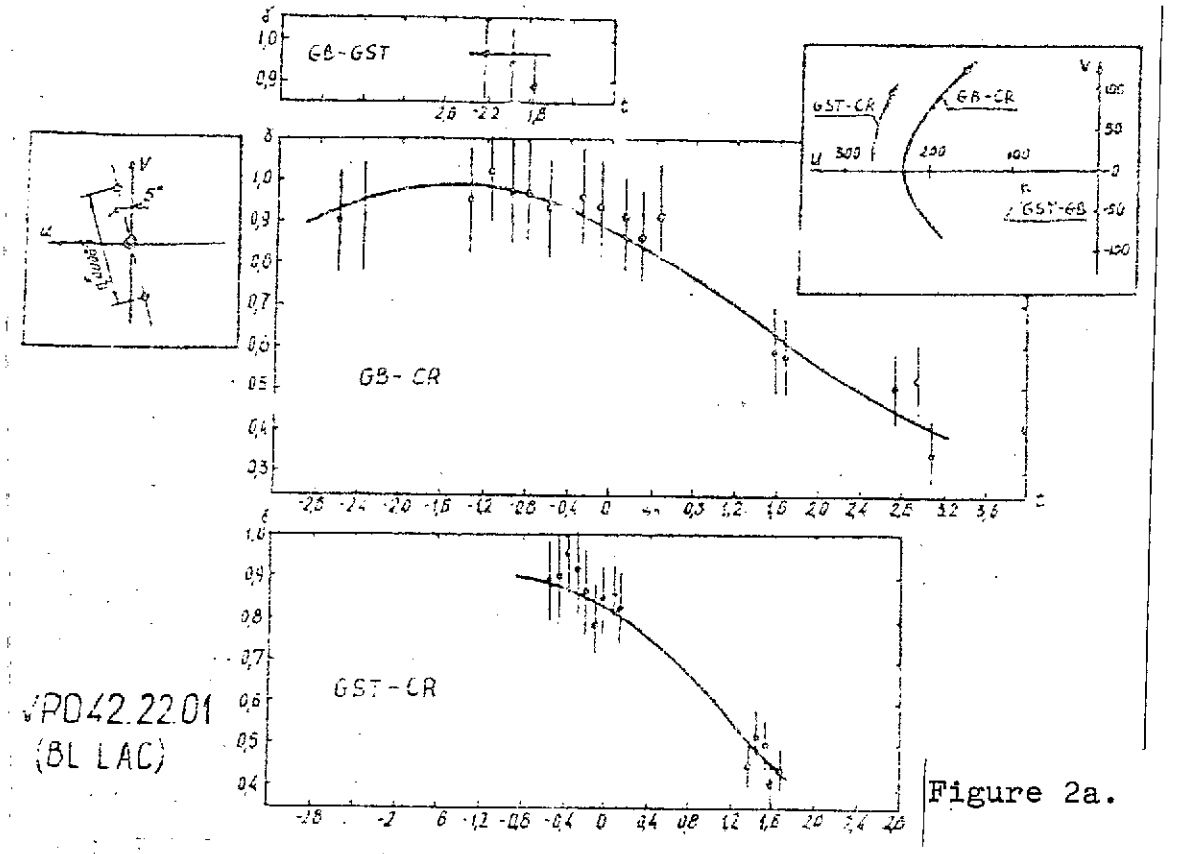

VP042.22.01
(BL LAC)

Figure 2a.

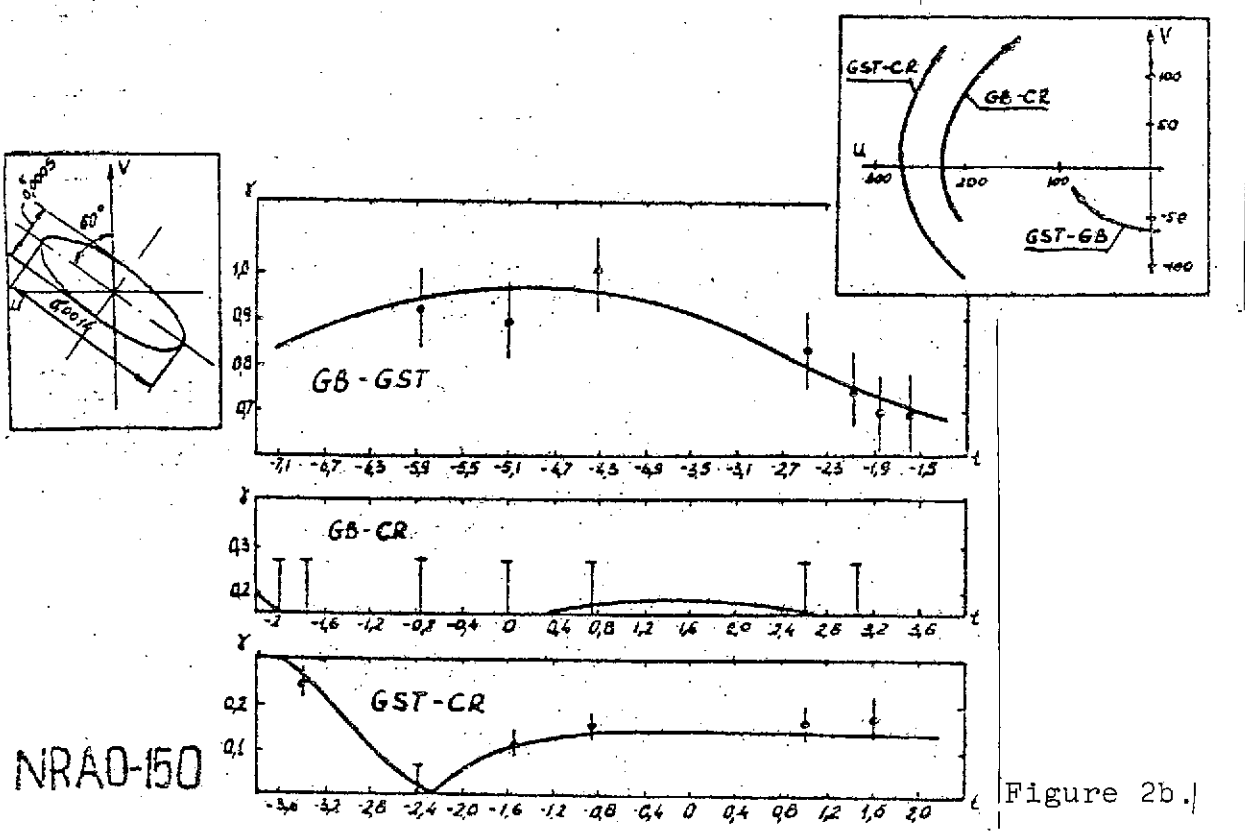

NRAO-150

Figure 2b.

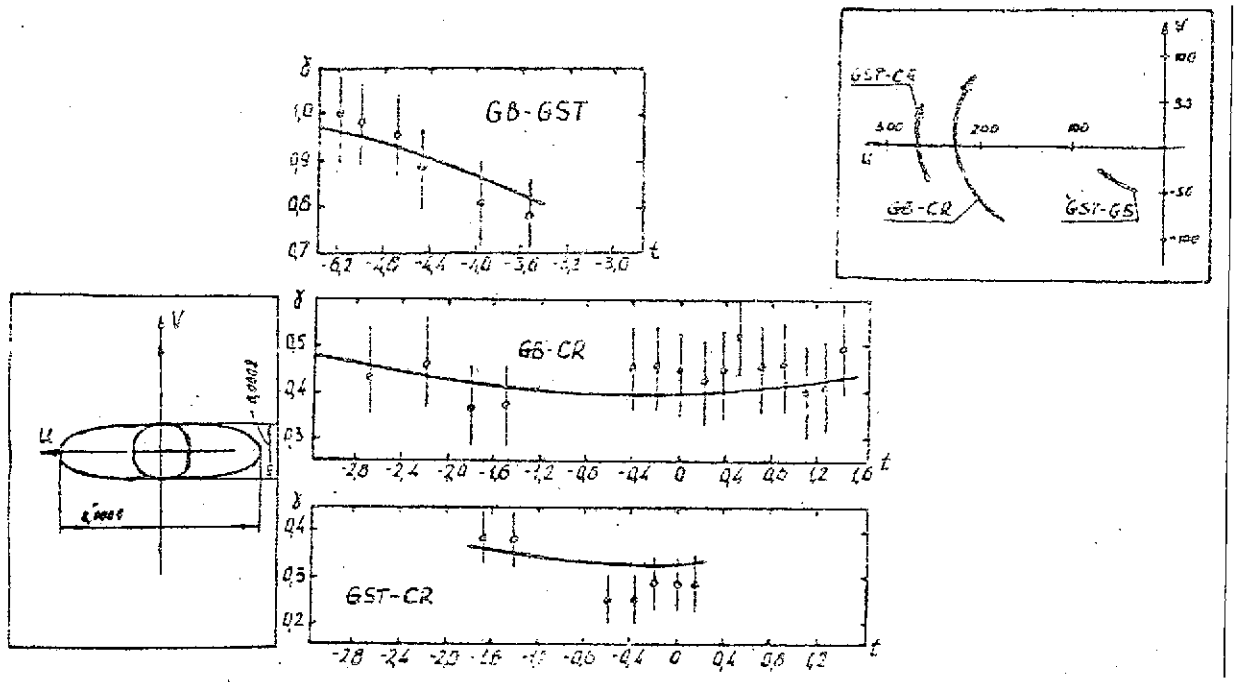

Figure 2c.

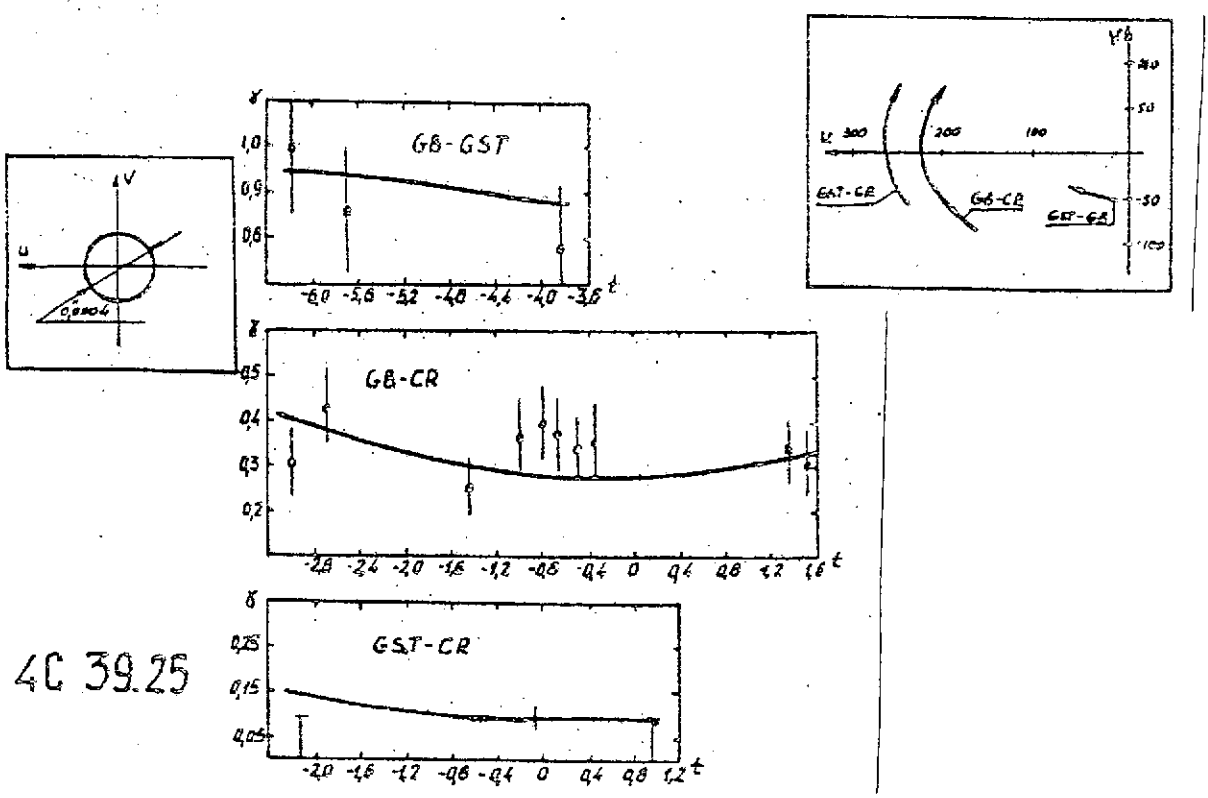

Figure 2d.

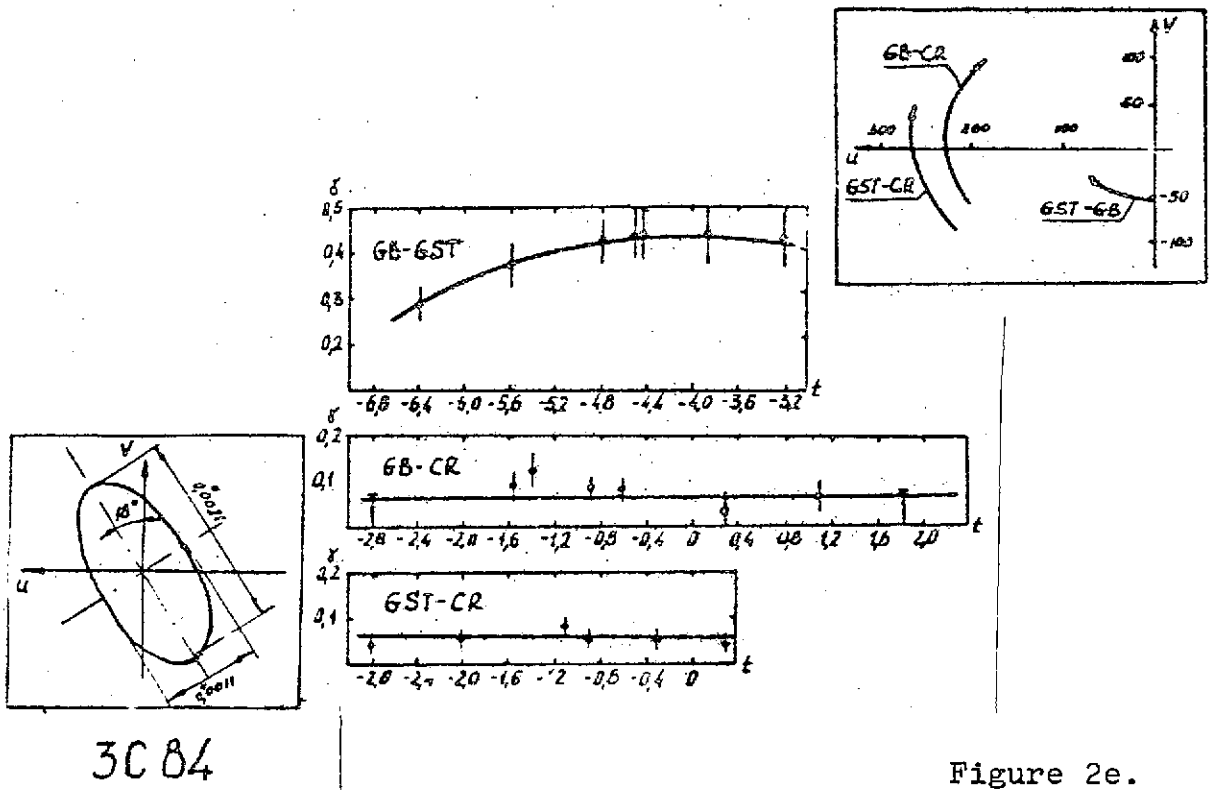

Figure 2e.

Figure 2. Visibility functions of the radio sources.

At the upper right are shown the projections of the three baselines on the source plane. The quantities U and V are plotted in millions of wavelengths. On the left are given the models of the radio sources which give the best agreement with the experimental results.

a — VRO 422201; b — NRAO 150; c — 3C345; d — 4C3925; e — 3C84.

models themselves are given on the left side in these figures. The dimensions for ellipses with the Gaussian distribution are given in cross section at the $1/e \simeq 0{,}62$ level.

The computations were carried out on the BESM-4 computer of the USSR Academy of Sciences Institute of Space Research. The structures of the compact components of the investigated sources derived as a result of these calculations are presented below.

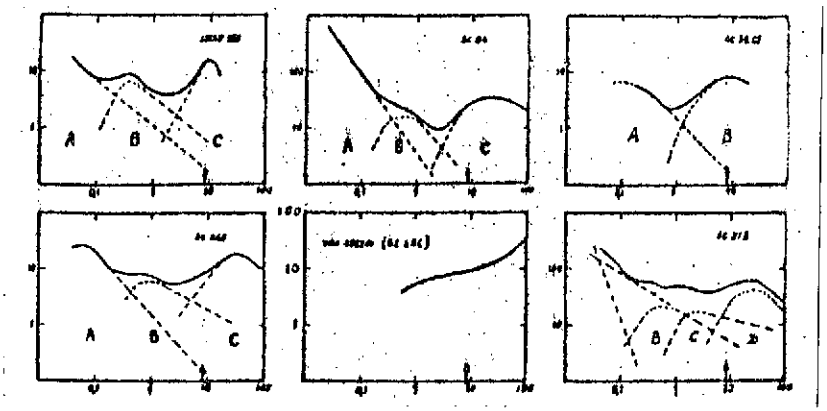

Figure 3. Spectra of the radio sources.

Frequency in Gegahertz is plotted along the horizontal axis, and the flux density in units of f.u. is plotted along the vertical axis.

1. OJ287

The radio source OJ287 has been identified with an optically visible object [8] — a quasar. Very active processes are occurring in it, which cause a rapid variability of its emission both in the optical region and in the radio region. The flux from this source varies in a number of cases in the course of a few days (Figure 4) [9, 10], which indicates the presence in it of components of exceedingly small angular dimensions. The spectrum of OJ287 is not known exactly, but it can be represented approximately in the form of Figure 5. Assuming the synchrotron /14 mechanism for the emission, one can distinguish two components A and B (indicated by a dashed line) in the spectrum. In this case the angular dimensions θ of the source are determined by the following relationship [13]:

$$\theta = 1{,}4 \cdot 10^{-2} F^{1/2} \nu^{-5/4} H^{1/4} (1+z)^{1/4}, \quad (1)$$

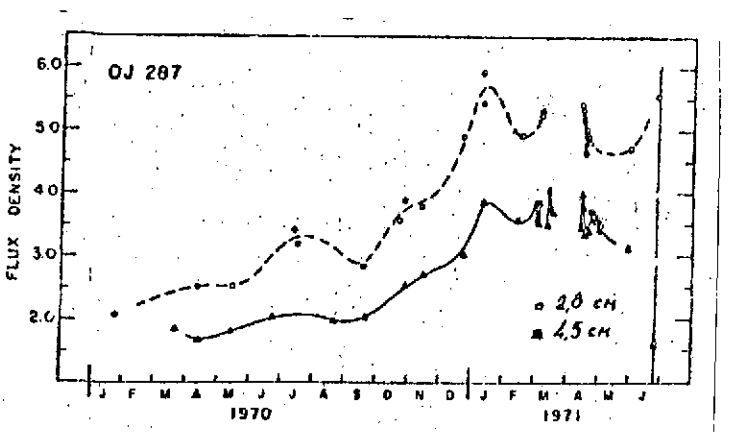

Figure 4. Variation of the flux of the source OJ287 1970-1971. The day of the observations, June 25, 1971, is denoted by an arrow.

where θ is in seconds of arc, F is the magnitude of the maximum flux in flux units, ν is the cutoff frequency in Gigahertz, H is the strength of the magnetic field in oersteds, and z is the red shift. The component A has a point of inflection at a frequency of about 1 GHz. The flux density at this frequency is approximately 1.5 f.u. We will subsequently assume the strength of the magnetic field to be $\sim 10^{-4}$ oersteds. It follows from Equation (1) that the dimensions of component A are approximately equal to ~0".002. The contribution by this component to the radio emission at the wavelength of 3.55 cm does not exceed 0.4 f.u., as is evident from Figure 5. Component B is younger, the point of inflection in its spectrum is encountered at millimeter wavelengths, and the maximum value of the flux density is ~10 f.u. In this case the angular dimensions of component B should be no more than 0".00003. As is evident from Figure 4, the flux density at wavelengths of 2.8 and 4.5 cm has increased significantly from the middle of 1970. One can assume that up to the moment of observations the spectrum of component B was shifted in the direction of lower frequencies (dot-dashed curve in Figure 5), whereupon its angular dimensions should be no greater than 0".00015, in agreement with Equation (1). The flux density of its radio emission at a wavelength of 3.55 cm was approximately 3.6 f.u. at the time of the observation. As is evident from Table 1, the source OJ287 has an identical correlated flux component at all three baselines, i.e., it remained unresolved even

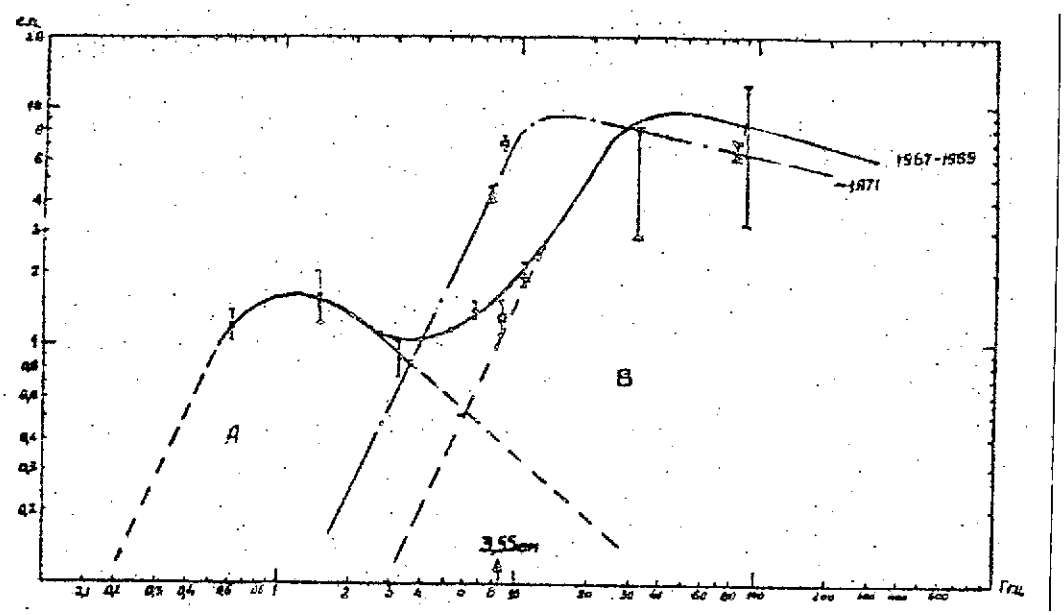

Figure 5. Spectrum of the radio flux 0J287 plotted on the basis of the following data:

x - [28], o - [12], □ - [11], ✕ - [9], • - [5].

at the maximum baseline (D_{max} = 270·10^6 λ), and consequently, its dimensions do not exceed 0".00025. This result corresponds /15 to the size of component B. Component A is resolved even from the minimum baseline of Goldstone-Green Bank, notwithstanding the fact that its contribution to the radio emission is small.

The present result corresponds to an estimate of its angular dimension based on the source spectrum and refines the experimental results at a nearby wavelength [5]. The brightness temperature of component B exceeds 2·10^{12} ° K.

2. OR103

This radio source is evidently a quasar. The flux density of its radio emission does not vary significantly [7]. It is not resolved on the Green Bank-Goldstone baseline, and the visibility function decreases to $\gamma = 0.77$ on the Goldstone-Crimea baseline, from which it follows that its size is equal to 0".00034 on the assumption of a uniform disc. In this case the brightness temperature is equal to $T_{br} = 6 \cdot 10^{11}$ ° K. Its size is $\theta < 0".0009$ at a wavelength 3.8 cm [5].

3. OK290

This source is evidently a quasar. Its flux density was practically constant in 1971 [7]. It was not resolved on the Goldstone-Green Bank baseline, and $\gamma = 0.56$ and 0.47 were obtained on the Goldstone-Crimea baseline for $D/\lambda = 254 \cdot 10^6$ and $D/\lambda = 266 \cdot 10^6$, which corresponds to a circular disc with a diameter of 0".0005 and $T_{br} = 1.5 \cdot 10^{11}$ ° K. The present result refines a conclusion drawn in the reference [5], in which an upper limit to the source angular size was derived at a nearby wavelength ($\lambda = 3.8$ cm) to be $\theta \leq 0".0008$.

4. OQ208

This source (a Seyfert galaxy) has a spectrum with a discontinuity at the frequency ~5 GHz [27]. The flux density at this frequency is equal to 3 f.u. It follows from Equation (1) that there is in this source a compact component with dimensions /16
~0".0003. The experimental results of this paper correspond to a model in the form of a circular disc with a diameter of 0".0018 ($l = 2.84$ pc), its flux equal to 1.5 f.u., and a nucleus with

dimensions < 0".00025 (l = 0.38 pc) with a flux of 1 f.u. This model agrees well with the value $\gamma = 0.64$ derived from the Goldstone-Haystack interferometer with $D/\lambda = 71 \cdot 10^6$ ($\lambda = 3.8$) [5]. The brightness temperature of the disc is equal to 10^{10} ° K and exceeds $3 \cdot 10^{11}$ ° K in the nucleus.

5. VR042.22.01 (BL Lac)

Powerful explosive processes resulting in a rapid variation of its radio emission intensity occur in this object (a compact galaxy) [7, 14].

The rapid variability of this source (Figure 6) [7, 14], and also the spectrum which rises right up to the millimeter waves (Figure 3) [15], is due to the high activity and must be associated with a rather complex structure and the existence of compact components of exceedingly small angular dimensions.

The experimental data on this source (Figure 2a) show a noticeable variation of the visibility function as a function of the hour angle for the Goldstone-Crimea and Green Bank-Crimea baselines, while at the same time the length of the baseline projection onto the U-V plane is practically unchanged. This circumstance indicates the extended nature of the source. The experimental values of the visibility function are fitted best by a double structure with a distance between components of /17
0".0005 and a position angle of 185° or by an elliptical disc with a Gaussian brightness distribution of the same orientation and with dimensions of its axes 0".002 × 0".0005.

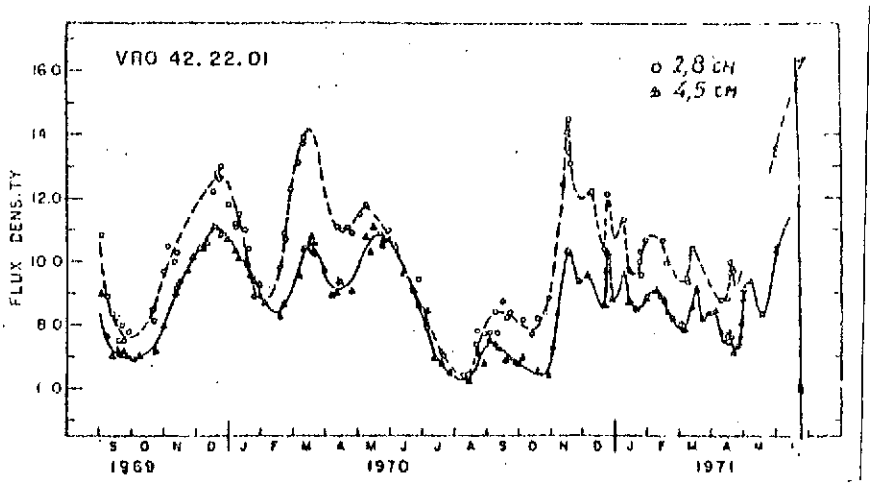

Figure 6. Variation of the flux of radio source VRO42.22.01 in 1969-1971. The day of the observations, June 25, 1971, is denoted by an arrow.

The rise in the source spectrum right up to millimeter wavelengths indicates the presence of bright components whose angular dimensions do not exceed 0".0001. Simultaneously, a second model for explaining the observed value of the flux in the millimeter wave region within the framework of the synchrotron theory (see Equation (1)) requires a magnetic field with a strength of ~10 oersteds, which is improbable. Therefore, the most preferable model is one consisting of two point components.

In February of 1971, the distance between the components in this source was equal to 0".0009, and the position angle was approximately the same [5], i.e., during the intervening time a "drawing together" of the components from 0".0009 to 0".0005 occurred. It is difficult to assume the reality of such a drawing together. It is more probable that a "change" in the distance is associated with the appearance during the indicated time of a third component or with a significant increase in its brightness. In May of 1971, an abrupt increase actually occurred

in the flux at centimeter wavelengths [7, 14], which can be explained by the formation of a new bright compact component.

As follows from Figure 6, the flux of this component at a wavelength of 3.55 cm was about 5 - 7 f.u. at the time of the observation. (The flux of this component can be found by assuming that it is equal to the increase in the total flux of BL Lac relative to the minimum level of April 20, which preceded the outburst.) It is natural to suppose that this position corresponds to the active nucleus of the galaxy, and the two older components are located symmetrically with respect to this center /18 at a distance of 0".00085 from each other and each has a flux of 3.4 f.u.

Such a three-component model agrees well, as is evident from Figure 2a, with the data obtained on all three baselines. Since the dimensions of the components do not exceed 0".0002, $T_{br} \geq 2.5 \cdot 10^{12}$ ° K in the central component and $T_{br} \geq 1.25 \cdot 10^{12}$ ° K in the outer components.

6. NRAO-150

This source has not been identified with any kind of optical object. It has a rather complex spectrum (Figure 3) in which three components can be distinguished [19]. In 1971 this source flux density at centimeter wavelengths did not undergo any rapid variations, and only a small rise was observed [7].

The angular dimensions of its components calculated on the basis of its spectrum [Equation (1)] are equal to θ_B = 0".012 and θ_C = 0".0003. The emission of component C dominates at

the wavelength of 3.55 cm. The experimental results are given in Figure 2b. The dependence of the visibility function on hour angle for the Goldstone-Green Bank and Goldstone-Crimea baselines indicates that the source has an extended structure, and the presence of a dip in the visibility function for the Goldstone-Crimea baseline at the time t = $2^h.4$ indicates that the source has either a double structure or a structure with a sharp brightness drop at the edges, for example, a uniform elliptical disc. Plots are presented in Figure 2b for the visibility function in the case of an elliptical disc with uniform brightness which includes within itself 89% (8.9 f.u.) of the flux of the entire source, with its axes having the dimensions 0".0014 × 0".0005 and with a position angle of 60°. The brightness temperature is equal to $3 \cdot 10^{11}$ ° K. The remaining 11% (1.1 f.u.) of the flux is emitted by components A and B, which are completely resolved at our baselines. The interferometric investigation of this source at a frequency of 1665 MHz [4] has shown that component B has dimensions equal to 0".015, but at a frequency of 5000 MHz [4] dimensions of 0".0013 were obtained for component C, which is in good agreement with our results. /19

7. 3C345

The source 3C345 is a quasar which has a complex spectrum (Figure 3) [15]. The dimensions of this component should, according to this spectrum, be equal to θ_A = 0".14, θ_B = 0".005, and θ_C = 0".0001, Approximately such dimensions for components A and B were obtained in the interferometric investigations at frequencies of 5000 MHz, 1665 MHz [16], and 400 MHz [17, 18].

The presence of a rather large correlated component on the Goldstone-Crimea and Green Bank-Crimea baselines and its significant variation on the Goldstone-Green Bank smallest baseline indicate that the source consists of two components with greatly differing dimensions. The analysis has shown that best agreement with the experimental points occurs in the case of a model consisting of an elliptical disc with a Gaussian distribution having dimensions for the axes of 0".0009 × 0".0002 (10.7 pc × 2.4 pc) and a nucleus 0".0002 in diameter (2.4 pc). The major axis of the ellipse is oriented along the U axis (position angle 90°) (Figure 2c). Both components have approximately the identical flux of 4.5 f.u. with $T_{br} = 2.5 \cdot 10^{11}$ ° K and $1.5 \cdot 10^{12}$ ° K for the large and small components, respectively. The remaining 12% (1.2 f.u.) of the flux pertains to the components resolved on all three baselines, i.e., having dimensions > 0.004 (components A and B).

The interferometric investigations of this source at a similar wavelength (λ = 3.8 cm) [5] showed that it can be represented in the form of two models: (1) a double-point model with a distance of 0".00086 between the components and (2) an elliptical disc with axial dimensions of 0".00095 × 0".00045. The position angle for both models is 103°. The visibility function of the double-point model should have been a minimum on the Green Bank-Crimea and Goldstone-Crimea baselines, which was not detected. The second model is in better agreement with the results of this paper. /20

8. 4C39.25

The flux density of this source's radio emission increases regularly at centimeter wavelengths, and only smooth flux variations with time are observed [7].

A bend occurs in the spectrum (Figure 3) of this quasar at a frequency of ~10 GHz, which corresponds to an angular size of ~0".0003. A disc model with a Gaussian brightness distribution having a diameter of 0".0004 (5.6 pc) agrees rather well with the experimental data (Figure 2d), and $T_{br} \approx 1.6 \cdot 10^{12}$ ° K. A value of $\gamma = 0.79$ for the visibility function is derived in the reference [5] at a baseline value of $85 \cdot 10^6 \lambda$ ($\lambda = 3.8$ cm), which is in good agreement with the present results. This component has a size $\leq$ 0".0004 at a wavelength of 6 cm [4].

9. 3C84

The flux density of this source (a Seyfert galaxy) increases constantly, and at the end of 1970 an increase in the growth of the flux was noted [7]. All of this indicates continual active processes occurring in the galaxy nucleus. The angular dimensions of the compact components should in this respect be very small. The source spectrum is complex (Figure 3) and consists of three main features [19], corresponding to separate spatial components. Components A and B have dimensions of 5' and 0".02 /21 [16] and are completely resolved at all three baselines. The observational results pertain in this respect to two components C, which is assigned in [16] the shape of a disc with a diameter of 0".0025. Best agreement with the experimental data is given by a model consisting of an elliptical disc with a Gaussian brightness distribution which contains 94% (40 f.u.) of the flux and has axial dimensions of 0".0021 × 0".0011 (0.72 × 0.38 pc) and a position angle of 17°, and of a component ($\theta < 0".00025$, [3.2 light months]), unresolved at all our baselines which contains 6% (2.5 f.u.) of the entire flux (Figure 2e). The brightness temperatures of the extended component and the nucleus are equal to $2.5 \cdot 10^{11}$ ° K and $7 \cdot 10^{11}$ ° K, respectively.

10. 3C273

This quasar has a variable flux density at millimeter and centimeter wavelengths [2, 7, 12]. The variation in its flux density at three-centimeter wavelengths occurs in a number of cases in the course of several months, which corresponds to an unusually small angular size of the components on the order of 0".00005. During the period of our observations, no kind of significant active variations were observed.

The source spectrum is complex and consists of several components (Figure 3) [19]. The dimension of the high-frequency component D is equal to ~0".0001, in agreement with Equation (1). This size pertains to some average active region, whose individual components may have significantly smaller angular dimensions and corresponds to the estimate derived above. Component C has an angular size of ~0".0015.

Interferometric investigations at longer wavelengths have shown that components B, C, and D have dimensions of 0".022, 0".002, and <0".0004, respectively [4].

A model consisting of a disc whose dimensions are equal to 0".0025 (7.9 pc) and a flux of 22 f.u. and two compact components having dimensions of <0".00025 situated inside the disc and spaced 0".0015 (4.7 pc) apart give the most satisfactory agreement with the results of this paper. The flux density of the radio emission of each of these components amounts to 4.4 f.u. The disc dimensions are in good agreement with the dimensions of component C indicated above. The double-point structure evidently pertains to component D. The brightness temperatures of the disc and nucleus are equal to $T_{br} = 8 \cdot 10^{10}$ and $1.5 \cdot 10^{12}$ ° K, respectively. Component B has two large dimensions and is resolved on all three baselines.

11. 3C120

Unusually powerful explosions occur methodically in this Seyfert galaxy, as a result of which its flux density varies abruptly. In particular, an increase in the flux occurred in the middle of 1970, after which it maintained a constant flux [7]. The spectrum of this object is complex and consists of several features, some of which are in the millimeter and centimeter wavelength region (Figure 3). A separation of the components in this source was detected in February - November 1971 with a speed exceeding the speed of light, namely, v/c = 2 [20]. Also just as in [20], two models were considered: a ring and a double structure. The models of the compact component derived at a different time are cited in Table 2 for comparison.

TABLE 2

Time		February 2, 1971 [20]	June 25, 1971 present results	November 3, 1971 [20]
Ring	Diameter, seconds of arc	0.0014	0.0018	0.0025
Double structure	Distance between components, seconds of arc	0.001	0.0013	0.0017
	Dimensions of the components, seconds of arc	<0.0005	0.0007	0.0013
	Position angle, degrees	95	85	85

The linear separation speed v of the components is related to the distance to the source D, its red shift z and the observed angular speed $\Delta\theta/\Delta t$ by the following relationship [21, 22]

$$v = \frac{c}{H} \frac{\Delta\theta}{\Delta t} z \Big/ (z+1)^2 \qquad (2)$$

where H = 75 (km/sec)·(Mpc)$^{-1}$ is Hubble's constant. /23

Substituting the data from Table 2 on the separation of the components in the double structure into Equation (2), we find that v = 1.6 C and 2.1 C for the February-June and June-November time intervals, respectively. Using Equation (2), the speeds with which the dimensions of the components increase, according to the same Table 2, are equal to >1.2 C and 3.1 C for the same time intervals, respectively. The fact of the excess of the observed speed of separation of the components in some sources has been discussed in the references [5, 20]. The results of this paper confirm the conclusions [20] that the speed of expansion of the components exceeds the speed of their separation. In addition, one can remark that during February through November of 1971 an accelerated separation and expansion of the components occurred in the source 3C120.

12. 3C274 /24

The radio source 3C274 is the gigantic elliptical galaxy M87, which contains a compact nucleus and an outburst in the form of an elongated blob of material. The spectrum of this radio source in the 10 - 5000 MHz region drops off and does not contain any features, and its spectral index is α = 0.81 [23]. Possibly the spectrum of the nucleus is more complex, but its relative contribution to the radio emission is small, and therefore it does not change the total spectrum of the source. The

latter fact may appear to be the reason for the absence of any kind of noticeable flux variations at centimeter wavelengths [7]. The radio interferometric investigations of the compact components at wavelengths of 13 and 3.8 cm [5, 24, 25, 26] have shown that there is a component in the nucleus with a diameter of 0".01 and a smaller component with a diameter of 0".001. The flux density of the radio emission of the small component increases with a reduction in the wavelength from 1 f.u. to 2 f.u. at wavelengths of 13 and 3.8 cm, respectively.

If this rise in the spectrum of the compact component is determined by reabsorption, the maximum should occur at a frequency of ~5 GHz, and the maximum value of the flux corresponds to ~2 f.u. In this case we find from Equation (1) that the size of the compact component should be equal to 0".0003. The value of the correlated flux on the Green Bank-Goldstone baseline amounts to 1.7 f.u., and the component is completely resolved on the other two baselines. Consequently, the compact component, which completely possesses the flux of 1.7 f.u., has a size of 0".001 (3.1 light months). This conclusion agrees well with that of the reference [5]. A certain discrepancy of the size derived with the size obtained above from the spectrum of the compact component may be explained by a magnetic field stronger than 10^{-4} oersteds in the source.

13. 3C144 /25

In the central part of the Crab Nebula there is located a compact source, namely, a pulsar. Interference fringes were not detected on any one of the three baselines, from which it follows that its flux is less than 0.8 f.u. or the dimensions of the compact source are larger than 0".003.

Conclusion

The results obtained indicate the presence in a number of the radio sources of compact components whose angular dimensions are less than 0".00025, i.e., less than the angular resolution attained at a wavelength of 3.55 cm on a baseline of maximum length under terrestrial conditions. Further increase in the angular resolution is possible only by means of reducing the wavelength or removing one of the elements of the interferometer to outer space. An increase in the angular resolution has fundamental significance in the investigation of the nature of the radiation of compact components.

As the observational results show, the brightness temperatures of the component whose angular dimensions exceed 0".001 are $10^{11} - 10^{12}$ ° K. This radiation may be explained within the framework of the synchrotron mechanism. At the same time, more compact components have brightness temperatures exceeding 10^{12} ° K, which introduces definite difficulties in explaining their nature [19]. In this respect, the dynamics of the components during the initial stages of the development is of special interest. To this end, regular observations are required both on baselines of the maximum length and also on intermediate baselines at a wide range of centimeter wavelengths. This approach permits studying the spectra of the components, their dimensions, the distances between them, and their time variation.

REFERENCES

1. Broderick, D. D., et al. Astr. Zh., Vol. 47, 1970, p. 784.

2. Kellermann, K. I. and I. I. K. Pauliny-Toth. Ann. Rev. of Astron. and Astroph., Vol. 6, 1968, p. 417.

3. Clark, et al. Astr. Zh., Vol. 49, 1972, p. 700.

4. Kellermann, K. I., et al. Ap. J., Vol. 169, 1971, p. 1.

5. Cohen, M. H., et al. Ap. J., Vol. 170, 1971, p. 207.

6. Kogan, L. R. Izv. VUZ'ov, Radiofizika, in press.

7. Medd, W. J., B. H. Andrew, G. A. Garvey, and J. L. Locke. Preprint Astroph. Branch NRCC, 1972.

8. Blake, G. M. Astroph. Letters, Vol. 6, 1970, p. 201.

9. Kinman, T. D. and E. K. Condin. Astroph. Letters, Vol. 9, 1971, p. 147.

10. Andrew, B. H., G. A. Harvey, and W. J. Medd. Astroph. Letters, Vol. 9, 1971, p. 151.

11. Gorshkov, A. G., et al. Astr. Tsirkulyar, Vol. 545, 1970.

12. Fogarty, W. G., E. E. Epstein, J. W. Montgomery and M. M. Dworetsky. A. J., Vol. 76, 1971, p. 537.

13. Slysh, V. I. Nature, Vol. 199, 1963, p. 682.

14. Macleod, J. M., B. H. Andrew, W. J. Medd and E. T. Olsen. Astroph. Letters, Vol. 9, 1971, p. 19.

15. Kellermann, K. I. and I. K. K. Pauliny-Toth. Astroph. Letters, Vol. 8, 1971, p. 153.

16. Kellermann, K. I., et al. Ap. J., Vol. 169, 1971, p. 1.

17. Broten, N. W., et al. M. N. R. A. S., Vol. 146, 1969, p. 313.

18. Clarke, R. W., et al. M. N. R. A. S., Vol. 146, 1969, p. 381.

19. Kellermann, K. I. and I. K. K. Pauliny-Toth. Ap. J., Vol. 155, 1969, p. L71.

20. Shaffer, D. B., M. H. Cohen, D. L. Jauncey and K. I. Kellermann, Ap. J., Vol. 173, 1972.

21. Sandage, A. R. Ap. J., Vol. 133, 1961, p. 355.

22. Sandage, A. R. Ap. J., Vol. 141, 1965, p. 1560.

23. Braude, S. Ya., I. N. Zhuk, A. V. Men', and B. P. Ryabov. Preprint No. 5, IRE of the USSR Academy of Sciences, 1969.

24. Kellermann, K. I., B. G. Clark, et al. Ap. J., Vol. 161, 1970, p. 803.

25. Broderick, J. J., et al. Ap. J., Vol. 172, 1972, p. 299.

26. Cohen, M. H., et al. Ap. J., Vol. 158, 1969, p. L83.

27. Andrew, B. H. and J. D. Kraus. Ap. J., Vol. 159, 1970, p. L45.

28. Kraus, J. D. and B. H. Andrew. Ap. J., Vol. 159, 1970, p. L41.

Translated for National Aeronautics and Space Administration under Contract No. 2483, by SCITRAN, P. O. Box 5456, Santa Barbara, California, 93108.